ELSEVIER

Journal of Molecular Catalysis A: Chemical 98 (1995) 9–14

JOURNAL OF MOLECULAR CATALYSIS A: CHEMICAL

Ozone decomposition and CO oxidation on CeO_2

A. Naydenov, R. Stoyanova, D. Mehandjiev

Institute of General and Inorganic Chemistry, Bulgarian Academy of Sciences, Acad. G. Bontchev Str., bl.11, Sofia 1113, Bulgaria

Received 8 April 1994; revised 2 August 1994; accepted 7 December 1994

Abstract

The reactions of ozone decomposition and CO oxidation by ozone on CeO_2 have been investigated. Kinetic experiments were carried out in a gradientless reactor. Ozone decomposition and CO oxidation were found to proceed in the temperature range 10–70°C. Using EPR, TPD and XPS spectroscopy, two different kinds of oxygen species are observed on the oxide surface, one of them being identified as O_3^-. It has been established that both oxygen species do not participate in CO oxidation. The oxidant in the low-temperature oxidation of CO is highly reactive atomic oxygen (probably O^-), which is produced by ozone decomposition on the oxide surface.

Keywords: Carbon monoxide; Cerium dioxide; Decomposition; Ozone

1. Introduction

Cerium dioxide is one of the most commonly used components in the three-way catalysts for neutralization of the automotive exhaust gases [1]. The CeO_2 acts as an 'oxygen store' during the lean operation conditions, while it can provide oxygen for H_2, CO and HC oxidation in the rich region [2–6]. It has been established that O_2^- radicals appear on CeO_2 during oxygen adsorption. On the other hand, the presence of Pt or Rh on the oxide surface leads to the formation of O^- radicals [7,8]. This difference is ascribed to the promoting role of the metal during oxygen dissociation. Treatment of CeO_2 with N_2O also leads to formation of O^- [9]. The studies have shown that O^- oxidation ability exceeds that of O_2^- and O^{2-} species. The interest in the mechanism of the heterogeneous catalytic decomposition of ozone on oxide surfaces and the possibility to use this reaction as a source of active oxygen for low-temperature oxidation of CO and organic compounds in waste gases has increased during recent years [10]. It should be pointed out that the publications are mainly in the patent literature, and there is no data about the reaction mechanism [11–15].

In previous investigations it has been proposed that the decomposition of ozone on transition metal oxides (α-Fe_2O_3, CuO, Co_3O_4, MnO_2) leads to the formation of atomic oxygen (probably O^-) on the oxide surfaces [16–20]. On the other hand, studies on the oxidation of CO and benzene in the presence of ozone have shown this form to be, most probably, the oxidant. Imamura and coworkers [10] reported the formation of atomic oxygen less negatively charged than O^{2-} in catalytic ozone decomposition on oxide surfaces. That is why the purpose of the present work is to investigate the reactions of heterogeneous catalytic decomposition of ozone on CeO_2 and the oxidation of CO in the presence of ozone. The catalyst chosen is CeO_2 because its properties

SSDI 1381-1169(94)00060-3

allow the use of EPR spectroscopy for the study of surface oxygen species. In addition, CeO_2 has a relatively weak catalytic activity in the oxidation of CO compared with the activities of CuO, Co_3O_4 and MnO_2 in the presence of molecular oxygen, which permits the elucidation of the role of ozone.

2. Experimental

2.1. Sample characterization

Commercially available CeO_2 (99%) was used for the experiments. The X-ray analysis was performed with a DRON-3 apparatus using CoKα radiation. The adsorption isotherm of N_2 was measured at 77 K with a volumetric apparatus. The specific surface area of the sample was determined by low temperature nitrogen adsorption using the BET method and was 130 m^2/g. The pore volume was 0.12 cm^3/g. The mesopore size distribution determined by the Pierce method [21] for the adsorption branch of the N_2 isotherm showed prevalence of pores with a size of 0.3 nm.

2.2. Kinetic investigations

The kinetic experiments were carried out in a gradientless reactor with external circulation. The reactor diameter was 15 mm. The gas flow at the inlet and outlet of the apparatus was 4.0 l/h. The circulation gas flow was 280 l/h. Commercial cylinders containing Ar (99.99%), O_2 (99.8%) and CO (99.997%) were used for the gas mixtures. The catalyst amount was 0.22 g (size 0.3–0.6 mm). The samples were treated beforehand in an Ar flow at 300°C for 3 h. The oxidation of CO by oxygen was investigated with a gas mixture containing CO within the concentration range of 7.91×10^{-2}–1.56×10^{-1} mol/m^3 in O_2 at temperatures 170–260°C. The oxidation of CO by ozone was investigated at inlet reagent concentrations based on the stoichiometric equation $CO + O_3 \rightleftharpoons CO_2 + O_2$. The gas mixtures were not diluted with argon because within the temperature range investigated (5–70°C) oxygen does not participate in ozone decomposition and CO oxidation. The decomposition of ozone was studied at an initial concentration of 3.27×10^{-1} mol/m^3. Ozone was synthesized from oxygen since when air was used, nitrogen oxides were formed in the ozone generator and they deactivate the oxide catalysts during the decomposition of ozone [16,17]. The reactions of ozone decomposition and CO oxidation in the presence of ozone were investigated in the temperature interval 10–80°C, because above 80°C the decomposition of ozone proceeds by a mixed homogeneous–heterogeneous mechanism. The CO and CO_2 analyses were performed with an on-line gas analyser (Infralyt 2106), O_3 being determined iodometrically.

2.3. EPR

The EPR spectra were recorded as the first derivative of the absorption signal using an ERS – 220 (former GDR) spectrometer within the temperature range of 100–400 K. The g-factor values were determined with respect to a DPPH standard. The signal intensity was calculated by double integration. The samples were treated in an ozone–oxygen flow at 5–65°C for 5–65 min.

2.4. XPS

The XPS spectra were recorded with an ESCALAB II electron spectrometer (VG Scientific) at a residual gas pressure in the analysis chamber of 10^{-7} Pa in the presence of a normal emission from a MgKα $-h\nu = 1253.6$ eV anode. At a pass energy of 50 eV, the resolution of the apparatus was about 1.4 eV as determined by FWHM of the Ag $3d_{5/2}$ peak. At 30°C the samples were treated in flows of O_2, $O_2 + O_3$, and $O_2 + O_3 + CO$, while at 200°C the flows used were of O_2 or $O_2 + CO$.

2.5. TPD

The TPD spectra were registered in an argon flow (3.5 l/h) at a pressure of 0.101 MPa and a heating rate of 7.5°/min. The amount of CeO_2

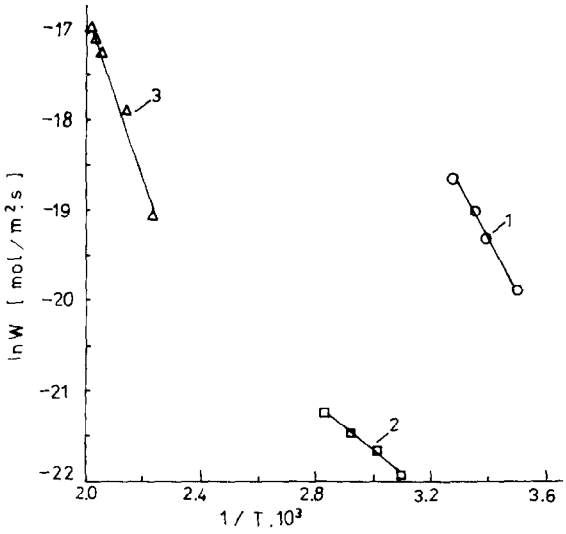

Fig. 1. Arrhenius plots of the reaction rates of ozone decomposition (line 1), CO oxidation by ozone (line 2) and CO oxidation by molecular oxygen (line 3).

samples was 1.0 g. The oxygen concentration was determined with an accuracy of 0.1 ppm using a Betatest OM 200 M apparatus. The apparatus is based on electrochemical principles.

3. Results

Fig. 1 presents the Arrhenius plots of the reactions of ozone decomposition (line 1), CO oxidation by ozone (line 2) and CO oxidation by molecular oxygen (line 3). The apparent activation energies of the decomposition of ozone and CO oxidation by ozone are 47 kJ/mol and 21 kJ/mol, respectively. The oxidation of CO by molecular oxygen proceeds at temperatures above 170°C with an apparent activation energy of 76 kJ/mol. Depending on the time and temperature of ozonation, the EPR spectrum of ozonated CeO_2 shows two kinds of signals (Fig. 2). One of them, denoted by A, represents a Gaussian line with $g = 2.0075$ and a line width of about 5 G. This signal appears after a relatively longer treatment of CeO_2 with O_2 (Fig. 2a). The second signal, denoted by B is anisotropic with $g_1 = 2.0124$, $g_2 = 2.0048$ and $g_3 = 2.0003$ ($g_{av} = 2.0058$), and appears at the beginning of the treatment (Fig. 2). In contrast to signal A, the g values of signal B depend on the conditions of treatment of CeO_2 with ozone: with rising temperature and increasing time of heating the anisotropic signal B ($g_1 = 2.0124$, $g_2 = 2.0048$ and $g_3 = 2.0003$) is transformed into a signal with axial symmetry ($g_{\parallel} = 2.0129$ and $g_{\perp} = 2.0024$), the average value remaining constant ($g_{av} = 2.0059$). In addition, both signals exhibit different thermal stabilities

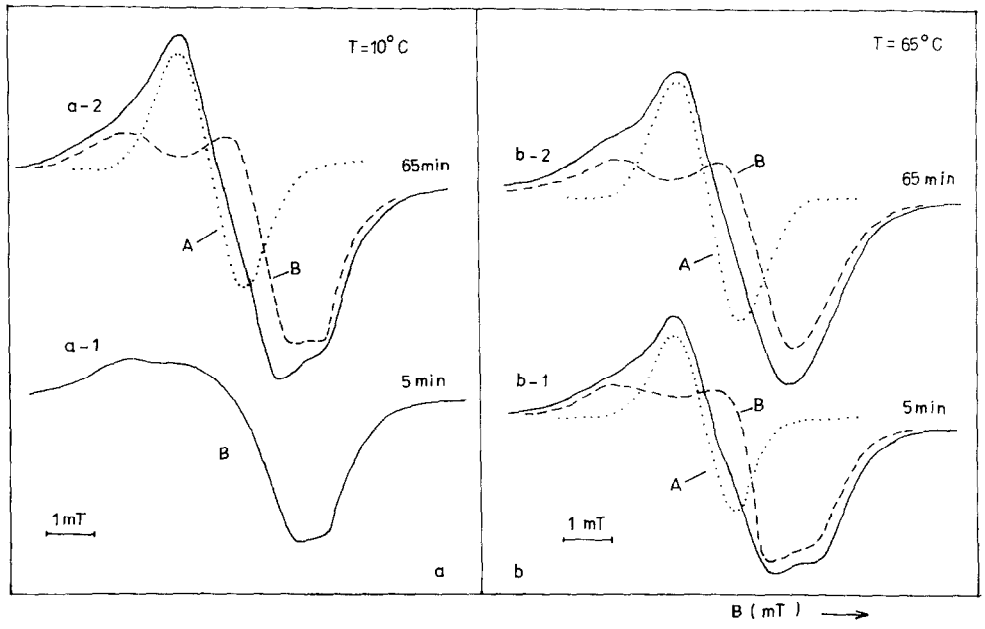

Fig. 2. EPR spectra at 100 K of CeO_2 treated with O_3 at (a) 10°C and (b) 65°C during 5 (a-1 and b-1) and 65 min (a-2 and b-2).

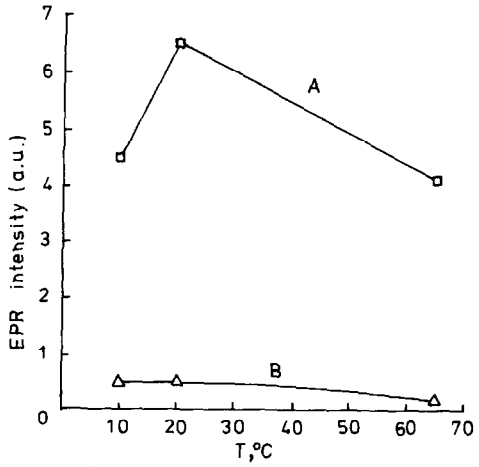

Fig. 3. Dependence of the A and B signal intensities on the temperature of treatment of CeO_2 with O_3.

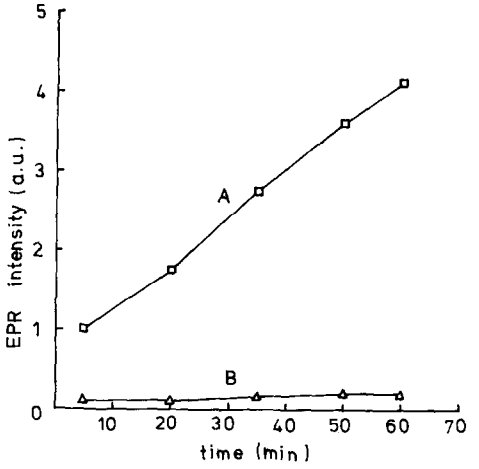

Fig. 4. Dependence of the A and B signal intensities on the time of treatment of CeO_2 with O_3 at 20°C.

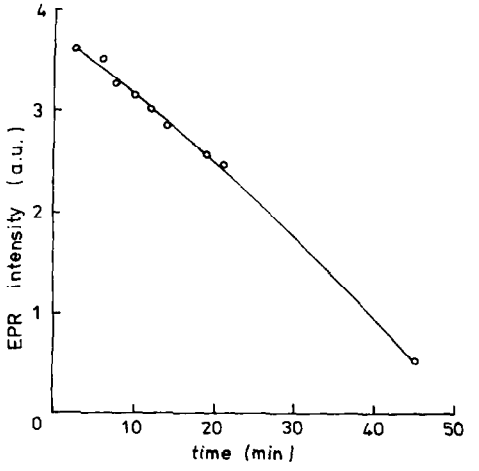

Fig. 5. Disappearance of signal B in Ar flow at 70°C.

(Fig. 3). It is evident that the A signal has a higher intensity at 20°C, while the intensity of the B signal decreases monotonously with rising temperature of CeO_2 treatment with O_3 (Fig. 3). Under isothermal conditions the intensity of signal A increases almost linearly with the time of treatment, while the intensity of signal B remains practically unchanged (Fig. 4). The treatment of previously ozonated CeO_2 with CO does not lead to any change in the shape and intensity of the EPR signal.

Treatment of CeO_2 with O_3 at 10–65°C for 5 to 65 min results in no EPR signals.

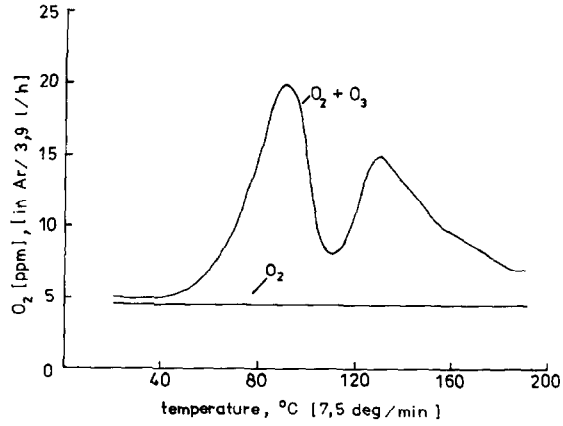

Fig. 6. TPD spectra of CeO_2 treated in O_2 and O_2/O_3 gas mixture at 30°C.

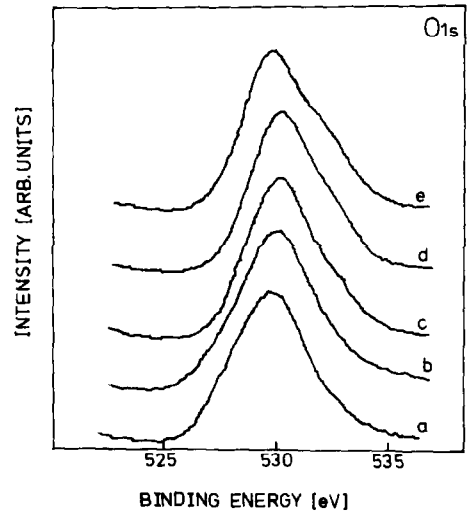

Fig. 7. XPS spectra of treated CeO_2 samples: (a) fresh CeO_2; (b) after treatment in O_2 flow at 30°C; (c) (O_2+O_3) at 30°C; (d) $(CO+O_2)$ at 200°C; (e) $(CO + O_3)$ at 30°C.

When the ozonated samples are treated in an argon flow, the intensities of the two signals decrease, B disappearing after about 50 min at 70°C (Fig. 5). It is worth noting that the vanishing of signal B is not accompanied by the appearance of new EPR signals. The TPD spectrum (Fig. 6) of CeO_2 treated with ozone at 30°C displays two oxygen peaks at 85 and 135°C, while in the absence of ozone no oxygen desorption is observed at 30–230°C. Fig. 7 shows the XPS spectra of CeO_2. When the sample is treated in a flow of O_3/O_2, there is a pronounced asymmetry at 532.4 eV in addition to the main O 1s peak at 530 eV which is typical of the oxygen from the oxide.

4. Discussion

According to the kinetic experiments a difference between the values of the apparent activation energies of CO oxidation by ozone(46 kJ/mol) and molecular oxygen (76 kJ/mol) were established. On the other hand, the oxidation by ozone proceeds at temperatures lower by 150°C. In this connection it may be suggested that oxygen with a high activity has appeared on the oxide surface during ozone decomposition, this leading to a difference between the reaction mechanisms. Based on the g value data, the anisotropic signal may be attributed to O_3^- radicals. The ground electronic state of the O_3^- radical is the B_1 state. According to the group theory of g values, the $g_{xy} > g_{xz} > g_e$ sequence is valid in this case. Irrespective of the fact that at higher temperatures of catalytic decomposition of ozone the symmetry of signal B changes from anisotropic to axial, the above sequence of g values is preserved in all cases. Summarizing, the g values of signal B correspond to O_3^- radicals whose amount depends on the time and temperature of treatment. After heating in an argon flow, O_3^- is desorbed without formation of new radicals. In contrast to the anisotropic signal, the symmetric signal A characterized by a higher thermal stability cannot be identified explicitly. It should be noted that the symmetric signal with $g = 2.003$ and $H_{pp} \approx 3$ G has been observed during adsorption of O_2 or NO on TiO_2, SnO_2 and ZnO and is identified as O^- [22,23]. The discrepancy between the calculated g components for O^- and the g values of the symmetric signal as well as the absence of superfine splitting due to the ^{17}O isotope reject the above assumption and enable one to attribute the symmetric signal to O_4^- radicals [24]. In addition, this signal, according to Naccache et al. [25], may be due to conductivity electrons localized after O_2 adsorption. The higher thermal stability of the isotropic signal compared with the anisotropic one indicates that this model describes most probably the nature of the isotropic signal. In addition to EPR data, the TPD spectrum of ozonated CeO_2 reveals the presence of two surface oxygen species differing in their strength of bonds with the oxide surface. The weaker bound oxygen species is desorbed at 70–110°C (Fig. 5) where the intensity of the EPR signal of the O_3^- radicals (signal B) decreases (Fig. 4). This gives grounds to assign the weakly bound oxygen species to O_3^- radicals. Their appearance on the CeO_2 surface may be explained in terms of charge-transfer adsorption. In other words, the interaction of O_3 with electron-excess surface sites of CeO_2 leads to the formation of O_3^- radicals. In the simplest case these sites may be Ce^{3+} ions as observed experimentally in the XPS spectrum of CeO_2 in the present and other investigations [26]. This process might be presented schematically as follows:

$$Ce^{3+} + O_3 \rightarrow [Ce^{4+}\ O_3^-]$$

Moreover, no interaction is established between adsorbed O_3^- radicals and CO. When O_3^- is desorbed during heating in an argon flow, no new radicals appear. These properties of O_3^- differ significantly from the properties of the well known O^- radicals [20]. It is known that O^- interacts with CO forming CO_2^- radicals [27]. When a $CO/O_3/O_2$ mixture is passed through CeO_2, no radicals originating from CO are observed, i.e., O_3 is the only constituent of the gas mixture that can react with the surface. This means that the decomposition of ozone precedes the oxidation of CO. On the other hand, the reaction $O^- + O_2 \rightarrow O_3^-$

occurs even when trace amounts of molecular oxygen are present and gives a new EPR signal which has been attributed to O_3^- [28–31]. Using data from the literature and our experimental results it may be suggested that the CO from the gas phase reacts directly with the atomic oxygen (probably O^-) produced on the oxide surface during the ozone decomposition in accord with the following reaction:

$$CO + [Ce^{4+}\ O^-] \rightarrow CO_2 + Ce^{3+}$$

i.e., the Eley–Rideal mechanism is possible.

5. Conclusion

On the basis of the results obtained it may be concluded that as a result of the heterogeneous catalytic decomposition of ozone on CeO_2 at 10–65°C, two kinds of oxygen species appear on the oxide surface – O_3^- and an unidentified species. The O_3^- has been characterized by a low thermal stability. It exists at temperatures below 70°C. It has been observed that both oxygen species do not participate in the low-temperature oxidation of CO. The existence of O^- has not been observed experimentally, but is logically suggested.

Acknowledgements

This work was supported by the Ministry of Science and Education.

References

[1] B. Harrison, A.F. Diwell and C. Hallett, Platinum Met. Rev., 32 (1988) 73.
[2] T. Shido and Y. Iwasawa, J. Catal., 136 (1992) 493–503.
[3] J.G. Nuhan, M.J. Cohn and J.T. Donner, Catal. Today, 114 (1992) 277–291.
[4] C. Binet, A. Jadi and J.C. Lavalley, J. Chim. Phys. Phys.-Chim. Biol., 89 (1992) 1779–1797.
[5] J.M. Schwartz and L.D. Schmidt, J. Catal., 138 (1992) 283–293.
[6] G.S. Zafiris and R.J. Gorte, Surf. Sci., 276 (1992) 86–94.
[7] L. Mendelovici, H. Tzehoval and M. Steinberg, Appl. Surf. Sci., 17 (1983) 175.
[8] J. Soria, A. Martinez-Arias, J.C. Conesa, G. Munuera and A. R. Gonzales-Elipe, Surf. Sci., 251/252 (1991) 990–994.
[9] S. Krzyzanowski, J. Chem. Soc., Faraday Trans. I, 72 (1976) 1573.
[10] S. Imamura, M. Ikebata, T. Ito and T. Ogita, Ind. Eng. Chem. Res., 30 (1991) 217–221.
[11] Jpn. Pat. No. 03 68,414 (1991), Daikin Industries, Ltd.
[12] Jpn. Pat. No. 03 67,277 (1991), Brother Industries, Ltd.
[13] Jpn. Pat. No. 03 98,618 (1991), Sakai Chem. Industries Co.
[14] Jpn. Pat. No. 03 143,524 (1991), Matsushita Electrical Ind.
[15] DE 4,007,964, 1991, Hager Klaus.
[16] A.Naydenov and D.Mehandjiev, Proc. 7th Int. Symp. Heterogeneous Catal. Burgas, 1991, pp. 1093–1097.
[17] D. Mehandjiev and A. Naydenov, Ozone Sci. Eng., 14 (1992) 277.
[18] A.Naydenov and D.Mehandjiev, Appl. Catal., 97 (1993) 17–22.
[19] A.Naydenov and D.Mehandjiev, CR Bulg. Acad. Sci., Tome 46, Vol.6, (1993) 49–52.
[20] A.Naydenov and D.Mehandjiev, 1st European Congress on Catalysis, Montpellier, 12–17 Sept. 1993, p. 117.
[21] C. Pierce J. Phys. Chem., 57 (1957) 149.
[22] T. Kwan, Proc. Int. Congr. Catal, 3rd, 1964, Vol. 1, p. 493.
[23] J.H.C. van Hooff, J. Catal., 11 (1968) 277.
[24] J.H. Lunsford, Catal. Rev., 8 (1973) 135.
[25] C. Naccache, P. Meriaudeau, M. Che and A.J. Tench, Trans. Faraday Soc., 67 (1971) 506.
[26] G.M. Ingo, G. Righini and L. Scoppio, Appl. Surf. Sci., 55 (1992) 257–267.
[27] C. Naccache, Chem. Phys. Lett., 11 (1971) 323.
[28] M. Che and A.J. Tench, Adv. Catal., 31 (1982) 77–133.
[29] A.J. Tench and T. Lawson, Chem. Phys. Lett., 7 (1970) 459.
[30] A.J. Tench, T. Lawson and J.F.J. Kibblewhite, J. Chem. Soc., Faraday Trans. I, 68 (1972) 1169.
[31] C. Naccache and M. Che, Proc. Int. Congr. Catal., 5th, 1972, Vol. 2, 1973, p. 1389.